The Infrared Nuclear Emission of Seyfert Galaxies on Parsec Scales: Testing the Clumpy Torus Models

Cristina Ramos Almeida[1], Nancy A. Levenson[2], Jose Miguel Rodríguez Espinosa[1], Almudena Alonso-Herrero[3], Andrés Asensio Ramos[1], James T. Radomski[4], Chris Packham[5], R. Scott Fisher[6] and Charles M. Telesco[5]

[1] Instituto de Astrofísica de Canarias, [2] University of Kentucky, [3] Instituto de Estructura de la Materia, [4] Gemini South Observatory, [5] University of Florida, [6] Gemini North Observatory

Abstract – submitted to ApJ

We present subarcsecond resolution mid-IR photometry from 8 to 20 μm of eighteen Seyfert galaxies obtained primarily from the Gemini Telescopes, representing one of the largest compilations of mid-IR Gemini observations of Seyferts. We construct spectral energy distributions (SEDs) with the unresolved mid-IR fluxes which are dominated by the AGN emission. At the spatial resolution afforded by Gemini, the fluxes are relatively uncontaminated by stellar emission. We augment the data with near-infrared measurements from the literature at similar angular resolution. We find that the IR SEDs of intermediate-type Seyferts are flatter and present higher 10 to 18 μm ratios than those of Seyfert 2 (Sy2) galaxies. We fit the SEDs with clumpy dusty torus models, which accurately reproduce the high spatial resolution measurements. For Sy2, we find the number of clouds along equatorial rays N_0 = 5-15, edge-on geometries more probable than face-on views, and the 10 μm silicate feature in shallow absorption. For the intermediate-type Seyferts, N_0 and the inclination angle of the torus are lower than those of the Sy2, with the silicate feature appearing in shallow emission or absent. The columns of material responsible for the X-ray absorption are larger than those inferred from the model fits, which is consistent with hot X-ray absorbing gas located within the dust sublimation radius whereas the mid-IR flux arises from an area farther from the accretion disc. In the models, the outer radial extent of the torus scales with the AGN luminosity, and we find the tori to be confined to scales less than 5 pc.

Sample and High Spatial Resolution Infrared observations.

The sample comprises 18 nearby Seyfert galaxies (12 Sy2, 2 Sy1.9, one Sy1.8, 2 Sy1.5 and one Sy1) for which we present ned new ground-based subarcsecond resolution mid-IR images. The data were taken in the N and Qa bands (~10 and 18 μm, respectively) with the instruments T-ReCS, Michelle and OSCIR on the Gemini and CTIO telescopes (an example is shown in Fig. 1). The mid-IR nuclear emission was determined using PSF subtraction. Near-IR nuclear fluxes of the same angular resolution from the literature were collected to construct high spatial resolution infrared SEDs (Fig. 2).

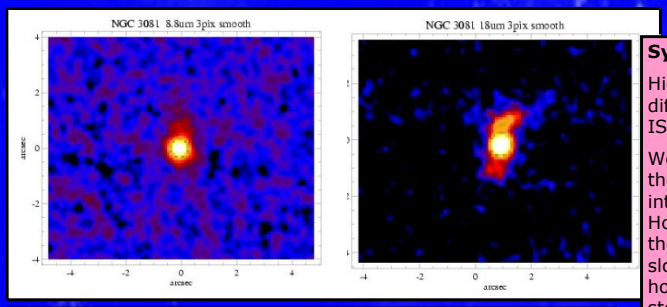

Fig. 1.- Example of mid-IR images in the Si2 and Qa filters of T-ReCS (8.8 and 18.3 μm, respectively) of the Sy2 NGC 3081. Note the enhanced extended emission in the Qa band image.

Sy1 versus Sy2 infrared SEDs.

High spatial resolution IR data provide SED shapes different from those of large apertura data SEDs (i.e., ISO, Spitzer or IRAS).

We found the slopes of the IR SEDs correlated with the Seyfert type in general. Sy2 show steep SEDs and intermediate-type Seyferts are flatter (Fig. 2). However, we find a range of spectral shapes among the Sy2, and also some int.-type SEDs have same slopes as Sy2. This cannot be reconciled with the homogeneous torus models, since they strictly predict steep SEDs for Sy2 and flat for Sy1. We do not observe such a strong dichotomy. Thus, we pursue clumpy torus models to reproduce the observed SEDs (see Table 1).

Galaxy	Type	α_{IR}	α_{NIR}	α_{MIR}
Centaurus A	Sy2	2.8±0.8	3.4±0.8	1.8±0.2
Circinus	Sy2	3.6±1.0	4.5±1.0	1.1±0.1
IC5063	Sy2	3.8±1.5	4.2±1.7	2.7±0.4
Mrk 573	Sy2	2.9±0.8	3.4±0.8	1.7±0.1
NGC 1386	Sy2	3.3±1.2	3.7±1.4	2.0±0.2
NGC 1808	Sy2	1.8±0.3	1.7±0.2	1.7±0.1
NGC 3081	Sy2	3.0±1.1	3.5±1.3	1.4±0.1
NGC 3281	Sy2	2.6±0.6	3.1±0.7	2.0±0.2
NGC 4388	Sy2	3.0±0.8	3.3±0.7	2.7±0.4
NGC 5728	Sy2	...	...	2.7±0.2
NGC 7172	Sy2	1.8±0.2	1.8±0.2	...
NGC 7582	Sy2	1.2±0.1	1.1±0.1	1.9±0.1
NGC 1365	Sy1.8	1.8±0.4	2.0±0.5	1.3±0.1
NGC 2992	Sy1.9	2.4±0.5	2.7±0.4	2.1±0.2
NGC 5506	Sy1.9	1.7±0.3	2.0±0.3	1.2±0.1
NGC 3227	Sy1.5	1.8±0.2	1.8±0.2	...
NGC 4151	Sy1.5	1.4±0.2	1.3±0.1	1.6±0.1
NGC 1566	Sy1	...	...	2.0±0.2

Tab. 1.- SEDs shape information. Fitted spectral indexes in the whole IR range (~1 to 18 μm), in the near-IR (~1 to 9 μm) and in the mid-IR (using the N and Qa data points).

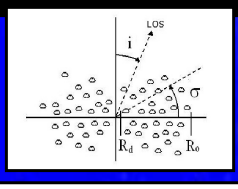

Fig. 3.- Scheme of the clumpy torus described in Nenkova et al. (2008a,b).

Tab. 2.- Clumpy model parameters and results from our fitting of the Sy2, Sy1.8 and 1.9 and Sy1.5.

Clumpy Model Parameters, Considered Intervals and Fitting Results

Parameter	Abbreviation	Interval	Sy2	Sy1.8 & 1.9	Sy1.5
Radial extent of the torus	Y	15	15	15	15
Width of the angular distribution of clouds	σ	[15°, 75°]	[50°, 75°]	[25°, 50°]	<35°
Number of clouds along an equatorial ray	N_0	[1, 15]	[5, 15]	[1, 7]	[1, 6]
Power-law index of the radial density profile	q	[0, 3]	...	[0, 2.5]	[0, 2]
Inclination angle of the torus	i	[0°, 90°]	>40°	...	<50
Optical depth per single cloud	τ_V	[10, 200]	<100	<110	~120

SED Modelling.

We fitted the IR SEDs of the Seyfert galaxies in the sample with the clumpy torus models of Nenkova et al. (2008a,b), shown in Fig. 3, using the BAYESCLUMPY code (Asensio Ramos & Ramos Almeida 2009). The results of the fitting are the probability distributions for the six free parameters that describe the clumpy models and the best fit to the observed SEDs (Figs. 4 and 5).

The clumpy models successfully reproduce the SEDs of both the Type 2 and the int.-type Seyferts, indicating that their IR SEDs are dominated by torus emission.

We find large number of clouds (N_0), broader tori and highly inclined views for Sy2, compared with those of int.-type Seyferts (Table 2), although the differences are not yet statistically significant. This suggests that Sy2 central engines would be blocked from direct view along more LOS than the int.-types and also that Sy2 tori would more efficiently reprocess the nuclear radiation (Table 3). **Are Sy1 and Sy2 tori intrinsically different?** More observations of Sy1 are needed to confirm these results.

SED fitting poorly constrain the radial extent of the torus because of the lack of high spatial resolution far-IR data, since the outer torus contains the coolest material.

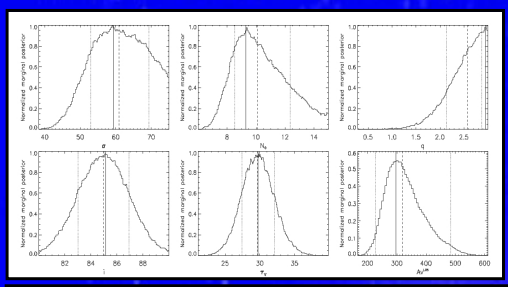

Fig. 4.- Probability distributions of the clumpy model parameters resulting from the fit of Circinus, together with the calculated value of the LOS Av. Solid, dashed and dotted lines represent the mode, the median and the 68% confidence interval around the median, respectively.

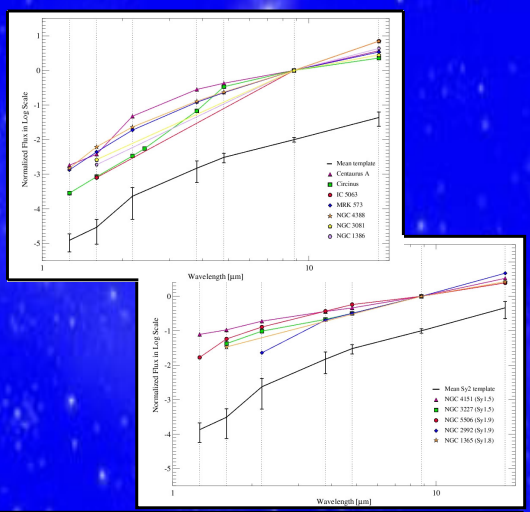

Fig. 2.- Top: IR SEDs for the 7 Sy2 with the highest resolution data (in colors) and resulting average template (solid black) shifted in the Y-axis for clarity. Bottom: IR SEDs for the int.-type Seyferts (in colors) and average Sy2 SED (solid black) for comparison. The SEDs have been normalized at 8.8 μm.

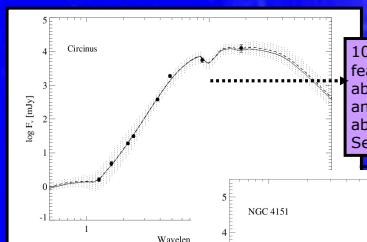

10 μm silicate feature in shallow absorption in Sy2 and in emission or absent in int.-type Seyferts.

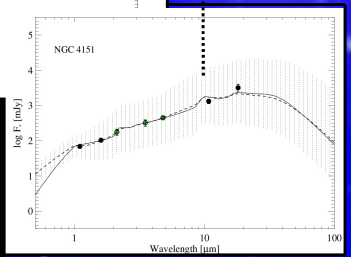

Fig. 5.- SEDs of Circinus (Sy2) and NGC 4151 (Sy1.5) fitted with the clumpy models. Solid and dashed lines represent models defined by the mode and the median of the histograms in Fig. 4. Shaded regions represent the range of models compatible with the 68% confidence interval.

Model predictions.

The columns of material responsible for the X-ray absorption are larger than those inferred from the model fits for most of the galaxies in the sample = the X-ray absorbing gas would be located within the dust sublimation radius ($R<R_d$, Fig. 3), while the mid-IR flux would arise from an area farther from the accretion disk.

In the models, the outer radial extent of the torus scales with the AGN bolometric luminosity (Table 3). Using $R_o=6x(L_{AGN}/10^{45})^{0.5}$ (fixing $Y = R_o/R_d = 15$) we find tori to be confined to scales less than 5 pc, in good agreement with other recent mid-IR observations.

Galaxy	L_{bol}^{AGN} (erg s^{-1})	L_{bol}^{tor} (erg s^{-1})	$L_{bol}^{tor}/L_{bol}^{AGN}$	R_o (pc)	L_{Xbol}^{AGN} (erg s^{-1})	L_{Xbol}^{AGN} / L_{bol}^{AGN}
Centaurus A	1.3×10^{42}	8.6×10^{41}	0.66	0.22	1.3×10^{43}	10
Circinus	1.0×10^{43}	8.1×10^{42}	0.81	0.60	1.2×10^{43}	1.2
IC 5063	2.4×10^{44}	2.1×10^{44}	0.87	2.94	1.7×10^{44}	0.7
Mrk 573	4.3×10^{44}	6.6×10^{43}	0.15	3.93	4.4×10^{44}	1.0
NGC 1386	3.4×10^{42}	2.0×10^{42}	0.59	0.35	1.3×10^{43}	4
NGC 1808	6.8×10^{42}	3.1×10^{42}	0.45	0.49	2.2×10^{41}	0.03
NGC 3081	1.0×10^{43}	8.9×10^{42}	0.89	0.60	1.0×10^{44}	10
NGC 3281	7.4×10^{43}	5.3×10^{43}	0.72	1.63	3.0×10^{44}	4
NGC 4388	2.1×10^{43}	1.7×10^{43}	0.81	0.87	1.5×10^{44}	7
NGC 7172	8.5×10^{42}	6.7×10^{42}	0.79	0.55	1.1×10^{44}	13
NGC 7582	1.1×10^{44}	1.1×10^{43}	0.10	1.99	9.8×10^{43}	0.9
NGC 1365	1.7×10^{43}	1.1×10^{43}	0.65	0.78	3.0×10^{43}	1.8
NGC 2992	2.8×10^{43}	1.5×10^{43}	0.53	1.00	3.0×10^{43}	1.1
NGC 5506	7.3×10^{44}	5.1×10^{43}	0.07	5.13	2.2×10^{44}	0.3
NGC 3227	2.0×10^{43}	1.1×10^{43}	0.55	0.85	3.8×10^{43}	1.9
NGC 4151	1.4×10^{44}	2.2×10^{43}	0.16	2.24	1.7×10^{44}	1.2

Tab. 3. – Model luminosity predictions (AGN and torus bolometric L), reprocessing efficiency, outer radius of the torus, X-ray bolometric luminosity and X-ray to mid-IR luminosity ratio.

References:

Asensio Ramos, A. & Ramos Almeida 2009, ApJ, 696, 2075

Nenkova, M., Sirocky, M., Ivezic, Z., Elitzur, M. 2008a, ApJ, 685, 147

Nenkova, M., et al. 2008b, ApJ, 685, 160